

Effect of Ga/Si interdiffusion on optical and transport properties of GaN layers grown on Si(111) by molecular-beam epitaxy

E. Calleja, M. A. Sánchez-García, D. Basak, F. J. Sánchez, F. Calle, P. Youinou, and E. Muñoz
Departamento de Ingeniería Electrónica, ETSI Telecomunicación, Universidad Politécnica, 28040 Madrid, Spain

J. J. Serrano, J. M. Blanco, and C. Villar*
Departamento de Tecnología Electrónica, ETSI Telecomunicación, Universidad Politécnica, 28040 Madrid, Spain

T. Laine, J. Oila, K. Saarinen, and P. Hautojärvi
Laboratory of Physics, Helsinki University of Technology, 02150 Espoo, Finland

C. H. Molloy and D. J. Somerford
Department of Physics and Astronomy, University of Wales, P.O. Box 913, Cardiff CF2, United Kingdom

I. Harrison
Department of Electrical and Electronic Engineering, The University of Nottingham, University Park, Nottingham NG72RD, United Kingdom

(Received 3 February 1998)

Optical and transport properties of wurtzite GaN layers, grown by plasma-assisted molecular-beam epitaxy on Si(111) substrates, have been investigated. An emission at 3.455 eV, analyzed by continuous-wave and time-resolved luminescence in undoped and Si-doped GaN layers, is assigned to excitons bound to Si donors with an optical binding energy of 50 meV. A common origin of this peak, for undoped and Si-doped GaN, is backed by secondary-ion-mass spectroscopy that evidences a Si diffusion from the substrate into the GaN layer for growth temperatures above 660 °C. Simultaneously, Ga diffusion into the Si substrate generates a highly *p*-type conductive layer at the GaN/Si interface, leading to unreliable Hall data in undoped and lightly doped layers. Positron annihilation reveals a concomitant vacancy cluster generation at the GaN/Si interface in samples grown above 660 °C. No traces of the “yellow band” are detected either in undoped or in Si-doped samples. [S0163-1829(98)00827-3]

I. INTRODUCTION

The origin and reduction of the residual *n*-type conductivity of undoped GaN layers grown on different substrates, by various epitaxial techniques, are still relevant issues. Depending on the residual *n*-type density, native-point defects (V_N) and/or contamination (O) were proposed as most probable candidates.¹⁻³ The reduction of the residual conductivity below 10^{17} cm⁻³, a current bottleneck for most growers, is needed to obtain efficient *p*-type doping with a low compensation and high mobilities, which is a key issue to achieve continuous-wave-laser operation through the reduction of the contact resistance and threshold current.⁴

Reliability of Hall data from GaN layers depends on many factors. Low resistivity Ohmic contacts, stable at low temperature, are easily achieved on *n*-type GaN but this is not obvious for *p*-type GaN. Besides, the layer morphology (columnar, grain boundaries, mixed cubic/hexagonal phases) might restrict parallel conduction leading to an apparent GaN insulating character, or, conduction may proceed through interfacial channels that mask the actual conductivity of the GaN layer. The formation of *p*-type inversion layers were already reported in AlN/Si(111) interfaces.⁵ Similar effects are expected in degenerated interface layers or in two-dimensional channels generated between the active layer and the buffer or substrate materials.⁶

We report on the Ga and Si diffusion at the GaN/Si(111) interface as a function of the growth temperature. Its effects on the transport and optical properties of undoped and Si-doped GaN layers are analyzed by Hall effect, continuous-wave and time-resolved photoluminescence (PL), secondary-ion-mass spectroscopy (SIMS), high-resolution x-ray diffraction (XRD), and positron annihilation spectroscopy (PAS). Although the results of this work might apply to GaN/AlN grown on SiC, where both Ga and Al are acceptors and N is a shallow donor,^{7,8} the high acceptor binding energies of Ga and Al in SiC make this potential problem less harmful.

II. EXPERIMENT

Wurtzite GaN films were grown by plasma-assisted molecular-beam epitaxy (MBE) on *p*-type Si(111) on axis substrates with 50–400 Ω cm resistivity. After native oxide removal at 850 °C for 20 min, a 7×7 reconstruction with Kikuchi lines indicated a high-quality surface. A cryogenically cooled rf plasma source (Oxford Applied Research CARS25) supplied the active nitrogen flow, which was kept constant throughout the growth. GaN layers, grown at 660–780 °C with a rf power of 550 W and a N₂ flow of 1 SCCM (SCCM denotes cubic centimeter per minute at STP) (growth pressure of 1.5×10^{-7} torr), had thicknesses between 0.8 and

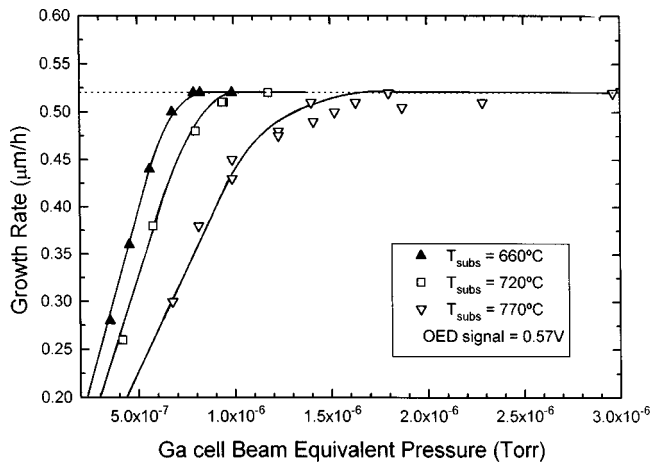


FIG. 1. GaN growth rate vs Ga flux (BEP) for different substrate temperatures and a constant active nitrogen flux. Solid lines are guides to the eye. All samples were grown without AlN buffers.

1.3 μm . Samples were grown either without buffer, or with an optimized AlN buffer layer.^{9–11} n -type doping was performed with a Si solid source.

Continuous-wave PL, excited with the 334-nm line of an Ar^+ laser, was measured with a Jobin-Yvon THR 1000 monochromator, a GaAs photomultiplier, and a lock-in amplifier. Time-resolved PL was measured with a frequency doubled Ti-sapphire laser with 200-fs pulses (peak power; 0.2 Mw/cm^2) pumped with a mode-locked Ar^+ laser, with a time resolution of 100 ps. Hall data were obtained as a function of the temperature (35–350 K) in a He closed-cycle cryostat using In dots or Ti/Al for Ohmic contacts. SIMS profiles were taken with O_2^+ ions as primary beam at 13 keV. XRD data were obtained with a BEDE D³ diffractometer. In PAS the Doppler broadening of the 511-keV annihilation radiation was measured using a variable-energy positron beam.

III. RESULTS AND DISCUSSION

A. Hall measurements in undoped GaN layers

Figure 1 shows the GaN growth rate versus Ga flux [beam equivalent pressure (BEP)] for different substrate temperatures and a constant amount of active nitrogen optical emission detector = 0.57 V).⁹ The growth rate increases linearly with the Ga flux until a saturation value is reached. The change in slope determines the stoichiometry point that delimits two distinct regions of growth, namely, under N-rich (linear) and Ga-rich conditions (saturated). Hall measurements were first performed at room temperature in undoped samples *without* AlN buffer layers, and Figs. 2(a) and 2(b) show the carrier concentration, conductivity type, and the mobility values as a function of the Ga flux and the growth temperature. All samples grown at around 660 °C are n type with increasing electron concentrations from 10^{16} to 10^{20} cm^{-3} , as a function of the Ga flux. Layer conversion from conductive to semi-insulating, driven by an increasing N flux, was already reported in MBE-grown GaN/Al₂O₃.^{12,13} We also found that a III/V ratio reduction leads to a sharp conductivity decrease and to semi-insulating layers. However, this effect might partially arise from a restricted parallel

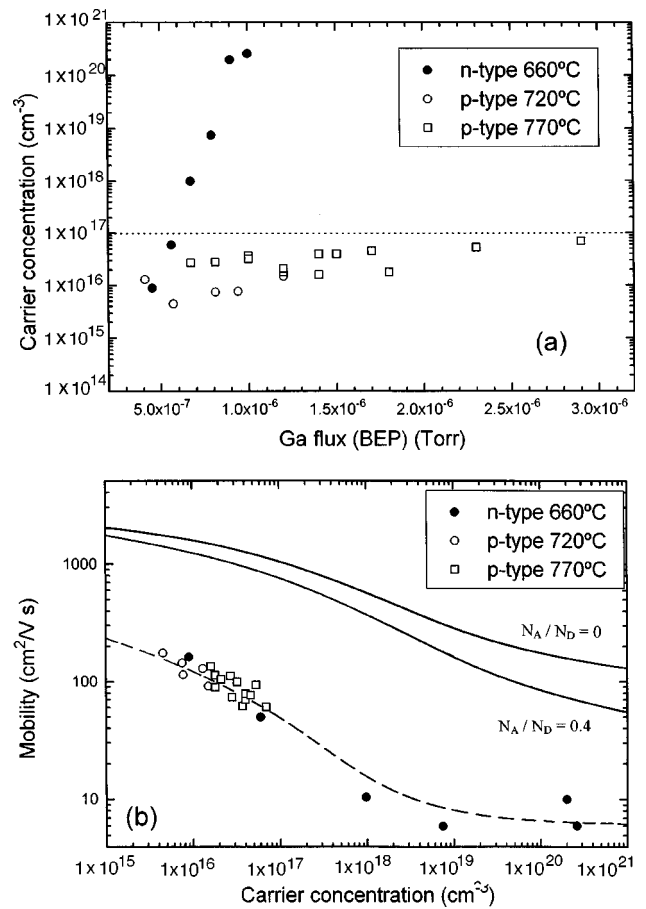


FIG. 2. (a) Room-temperature Hall-carrier concentration vs Ga flux for undoped GaN samples grown at different temperatures without AlN buffers. Above 660 °C all samples have a p -type conductivity. (b) Room-temperature Hall mobility versus carrier concentration in undoped GaN layers from (a). Solid lines are theoretical fits with N_A/N_D compensation ratios of 0 and 0.4 after Ref. 14. Dashed line is a guide to the eye.

conduction due to a columnar morphology, typical when growing under N-rich conditions.⁹ That may be the case of vanishing mobilities and high resistivities, together with excitonic PL emissions reported in GaN grown under N-rich conditions.¹² The electron mobility in Fig. 2(b) follows qualitatively the theoretical model,¹⁴ but it is ten times lower than that reported for GaN on sapphire.^{15,16} Compensation alone cannot account for such low mobilities, so that, a strong scattering process due to a high-dislocation density must be present. Indeed, these layers, grown *without* AlN buffer, were rather polycrystalline with full width at half maximum (FWHM) values, from XRD measurements, between 70 and 100 arc min. When the growth temperature increases to 720 °C the conductivity changes to p type, independently of the Ga flux, as shown in Fig. 2(a). Besides, for a given growth temperature, the longer the growth time, the higher the p -type conductivity; and a further increase of the growth temperature to 770 ± 10 °C leads to higher conductivity values, always p type.

Temperature-dependent Hall data in undoped GaN layers [Fig. 3(a)] lead to activation energies (E_D) from 9 to 21 meV for GaN grown by MBE on Si(111) at 660 °C (1); GaAs(111) (2); and by metal-organic vapor-phase epitaxy (MOVPE) on sapphire (3). The unintentional n -type conduc-

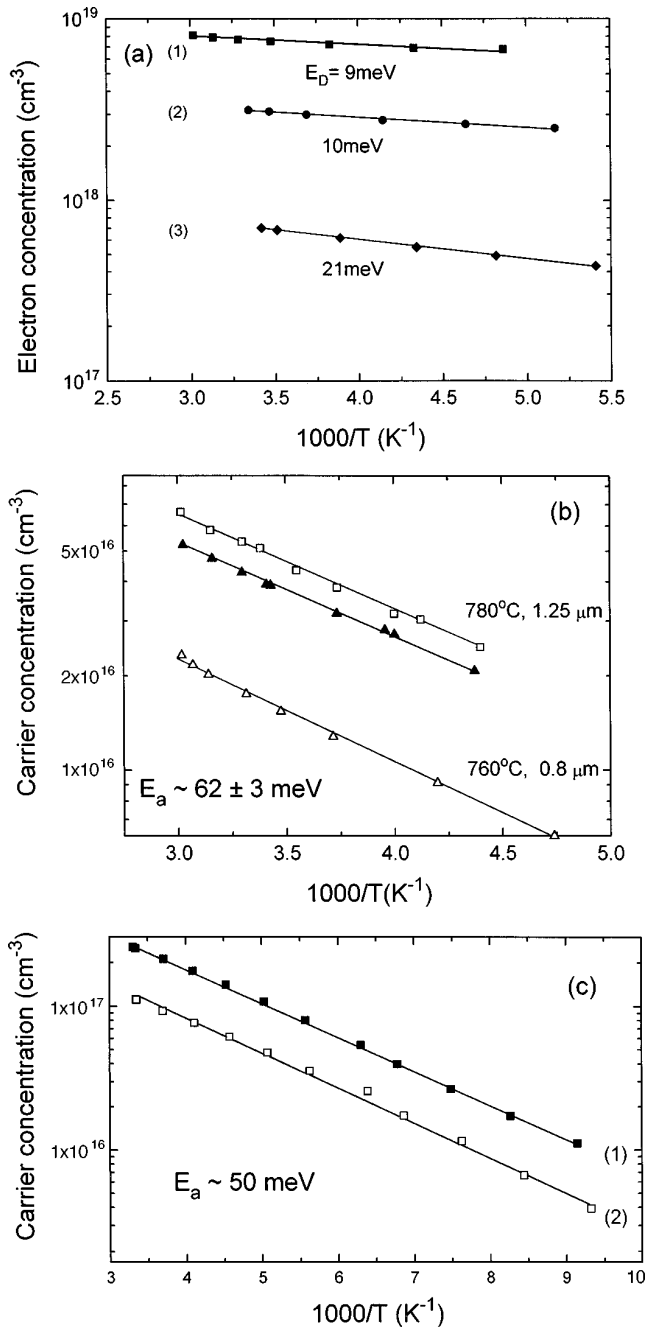


FIG. 3. (a) Temperature-dependent Hall data in undoped GaN layers grown with different techniques: MBE at 660 °C on Si(111) (1); MBE on GaAs(111) (2); and MOVPE on sapphire (3). (b) Temperature-dependent Hall data in undoped GaN layers grown on Si(111) at temperatures *above* 660 °C. Layer thickness (growth time) is also shown. (c) Temperature-dependent Hall data in an undoped AlN buffer (1) and an undoped GaN on an AlN buffer (2). Both AlN buffers were grown at high temperature (850–910 °C).

tivity of these samples is rather high and very much dependent on the growth method and conditions, as it has been often reported in the literature. The difference in donor-activation energies observed in these samples would suggest different residual contaminants or native defects, but a comparison cannot be straightforwardly done because of impurity-band formation for high-electron densities. Different activation energies for residual donors in GaN, at 20–36 meV (Refs. 13 and 16) from Hall data and 35 meV (Ref. 17)

from PL data, have been reported in undoped GaN samples. In our case, Hall data in Fig. 2(a) shows a very sharp conductivity increase with the Ga flux, and, since no conceivable oxygen source in the MBE system would reach such a high level (residual gas analysis did not show any O₂ trace), it follows that point defects like V_N or Ga₁, or complexes involving them, are most likely to be the origin of the *n*-type conductivity in our undoped GaN samples.

As pointed out before, undoped GaN samples grown by MBE *above* 660 °C show a *p*-type conductivity, with an activation energy (E_A) of 62 ± 3 meV [Fig. 3(b)] independent of the III/V ratio, growth temperature, and layer thickness, pointing to a common acceptor. Moreover, undoped GaN layers grown at 780 °C and thinned by dry etch with SF₆,¹⁸ or a thermal anneal of the Ohmic contacts at higher temperatures, reveal that the closer to the GaN/Si(111) interface, the higher the *p*-type conductivity (Table I). Since Ga is a shallow acceptor in Si, at some 65 meV above the valence band,¹⁹ and considering the activation energies shown in Fig. 3(b), we conclude that the Hall conductivity is dominated by a highly conductive *p*-type interface channel generated by Ga diffusion into the Si substrate. Assuming an *extrinsic* diffusion time of 2 h (growth time), and the Ga solubility limit and diffusion coefficient in Si at 800 °C being 2×10^{19} cm⁻³ and 10^{-16} cm²/sec, a rough estimate gives a *p*-type channel $\cong 300$ Å thick with an average hole density of 10^{19} cm⁻³. Mobility values in Table I also agree with the hole mobilities in Si for these acceptor densities.

The GaN-layer quality improves considerably when grown on optimized, high temperature (>800 °C) AlN buffers.^{9–11} We have checked the buffer-crystal quality and adequacy to further grow GaN by means of the FWHM of XRD rocking curves; surface roughness by atomic force microscopy (AFM); and surface reconstruction by reflection high-energy electron diffraction (RHEED). While XRD relates directly to monocrystallinity, AFM and RHEED also give information about the surface flatness (two-dimensional growth) and stoichiometry. Optimized AlN buffers show a FWHM of 10 arc min; a root-mean-square surface roughness of 46 Å, and a 2×2 RHEED reconstruction.^{9–11} Because Al behaves as an acceptor in Si and its diffusion coefficient is higher than that of Ga,¹⁹ a diffused *p*-type layer at the AlN/Si(111) interface is also expected. Hall data in Fig. 3(c) reveal that GaN layers grown on AlN buffers, as well as the AlN buffers alone, have *p*-type conductivities with an activation energy very close to that of the Al acceptors (57 meV) in Si.¹⁹ Although the AlN buffer layer should isolate the GaN top layer from the AlN/Si(111) interface, this seems not to be the case, even with unannealed Ohmic contacts. Look and Molnar²⁰ reported *n*-type highly conductive GaN interface channels due to a high density of stacking faults extending over 3000 Å from the GaN/Al₂O₃ interface. Thus, we speculate that a high-dislocation density in the AlN buffer might help electrical contact with the AlN/Si interface.

B. SIMS measurements in undoped GaN layers

SIMS spectra, with 13-keV O₂⁺ as primary species at 60° incidence, were taken in undoped GaN layers grown on high resistivity (>400 Ω cm) Si(111) *without* AlN buffers. Figures 4(a) and 4(b) show Ga and Si profiles in samples grown

TABLE I. Change in Hall data with sample thickness and annealing temperature in GaN/Si(111).

Sample thickness (μm)	$[p]$ (cm^{-3})	μ_p ($\text{cm}^2/\text{V s}$)	ρ ($\Omega \text{ cm}$)
0.77	3.6×10^{16}	100	1.72
0.51	6.0×10^{16}	94	1.21
0.15	2.2×10^{17}	89	0.32
Annealing temperature ($^\circ\text{C}$), 90s	$[p]$ (cm^{-3})	μ_p ($\text{cm}^2/\text{V s}$)	ρ ($\Omega \text{ cm}$)
Unannealed	3.5×10^{16}	101	1.72
380	3.8×10^{16}	97	1.68
450	4.2×10^{16}	91	1.63
500	5.1×10^{16}	77	1.57

at increasing temperatures. Besides an instrumental effect of “trailing etch” (slow exponential decay), an enhancement of Ga diffusion into the Si substrate, as well as of Si into the GaN layer, is clearly observed. The GaN/Si(111) interface was precisely determined from the O_2 signal change. It follows from Hall data that the p -type conductivity of samples in Fig. 4(a) increases with the Ga diffusion. Figure 5 shows an enhancement of Ga/Si diffusion that becomes very strong at high-growth temperatures, with complex profiles that remind an extrinsic diffusion followed by a redistribution process that might depend on the film compactness. Since the carbon signal keeps near the detection limit throughout the GaN layer and the Si substrate, it is likely not arising from the GaN layer. As pointed out before, Ga diffusion into the

Si substrate accounts for the apparent p -type conductivity of the GaN layers. On the other hand, diffused Si into the GaN layer acts as a shallow donor.

C. Photoluminescence measurements in undoped GaN layers

Although near-band-edge PL spectra have been analyzed in undoped GaN/Si layers,^{9,21,22} the origin of some emissions is still unclear. Free excitons dominate the luminescence of columnar, whiskerlike samples, whereas a weak and broad peak at 3.455 eV becomes dominant in compact layers because of a sharp excitonic-emission reduction,⁹ most likely due to the generation of a high density of dislocations in rather polycrystalline samples (no AlN buffer). The growth temperature does not affect the energy position of this peak (Fig. 6), but it enhances the emission intensity. The inset in

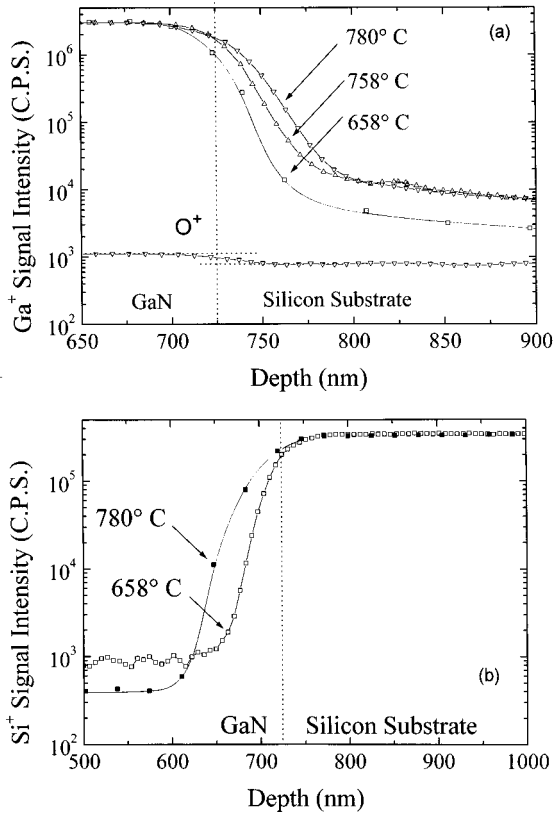


FIG. 4. SIMS profiles of Ga into Si (a), and Si into GaN (b), for different growth temperatures. As the Ga diffuses deeper into the Si (a), layer conductivity changes from n type (658 $^\circ\text{C}$) to increasing p type ($1.5\text{--}5.5 \times 10^{16} \text{ cm}^{-3}$ for 758 and 780 $^\circ\text{C}$).

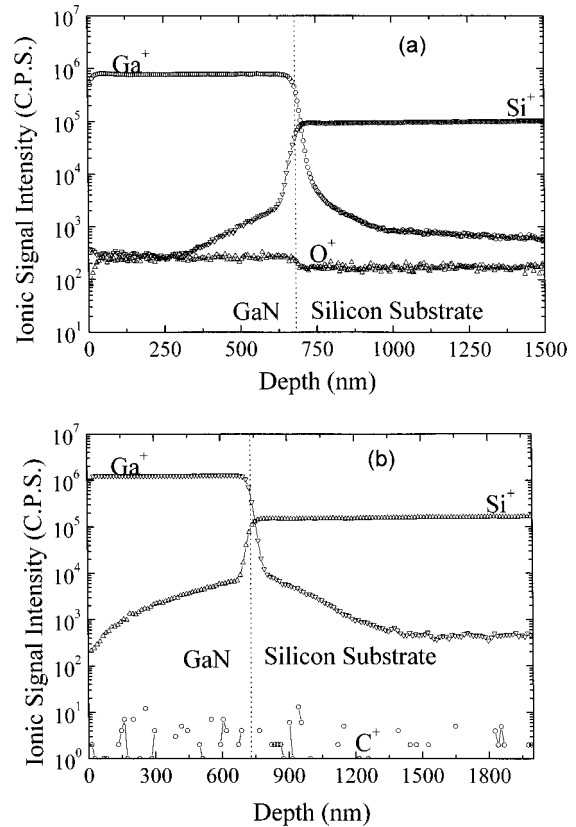


FIG. 5. SIMS profiles in GaN samples grown at 720 $^\circ\text{C}$ (a), and 780 $^\circ\text{C}$ (b).

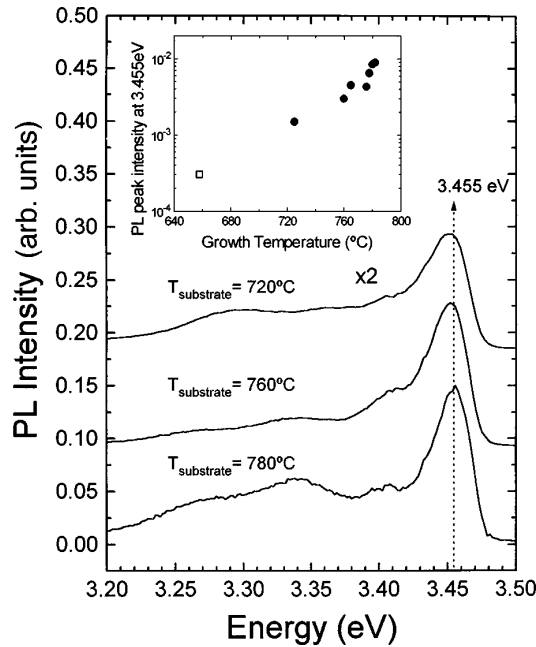


FIG. 6. PL spectra of undoped GaN layers grown on Si(111) without AlN buffer at increasing temperatures. The inset shows the PL intensity dependence on the growth temperature (see text). The open square corresponds to the same PL emission in a GaN layer grown at 660 °C. All spectra are shifted for clarity purposes, but they have the same baseline.

Fig. 6 shows data from a series of samples grown with different thicknesses and measured under various excitation densities, so that they are normalized, whereas spectra shown in this figure belong to selected samples grown in sequence under the same conditions, having similar thicknesses and measured under an identical excitation, thus allowing a straightforward comparison. Since a growth temperature increase leads to a higher and deeper Si diffusion into the GaN layer, it seems reasonable to establish a relation between the Si donors and the PL emission at 3.455 eV. Considering that compact GaN layers are under biaxial-tensile strain due to differences of thermal expansion coefficients between the epilayer and the substrate,²³ this emission can be assigned to the donor-bound exciton related to Si donors. The broad line shape of this excitonic emission might be understood as due to local-potential fluctuations and/or inhomogeneous-residual strain in the GaN layer, which are expectable in a polycrystalline material. Dominant and broad peaks at 3.455 and 3.460 eV, were attributed to donor-bound excitons of unknown origin in GaN layers grown on Si(111).^{24,25}

Figure 7 shows time-resolved PL decays, tuned at 3.455 eV [(a) and (b)], with fast exponential decays in compact GaN layers, either undoped (a) or Si doped (b). The lifetimes are about 160 ± 10 ps and they are almost identical to the measured lifetime of the donor-bound exciton at 3.472 eV, determined in a fully-relaxed, columnar GaN layer.²¹ It is also worth noting that the temperature dependence of the emission at 3.455 eV in undoped GaN layers follow that of the band gap up to 100 K where it fades out.²¹

Figure 8 shows low-temperature PL spectra corresponding to undoped GaN layers (1 μm thick) grown on optimized, high-temperature AlN buffers.^{9–11} As expected, the GaN crystal-quality improvement, resulting from a better-

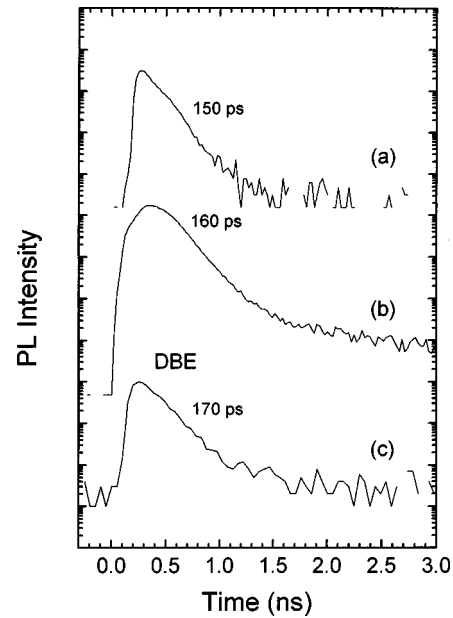


FIG. 7. Time-resolved PL spectra from several GaN layers: (a) undoped GaN at 780 °C without AlN buffer, tuned at 3.455 eV, (b) Si-doped GaN ($1.7 \times 10^{19} \text{ cm}^{-3}$) on an AlN buffer at 910 °C, tuned at 3.455 eV, (c) relaxed, undoped GaN at 780 °C without AlN buffer, tuned at 3.472 eV donor bound exciton.

ordered growth, is inferred from XRD data showing a best FWHM value of 8.5 arc min.¹⁰ The GaN optimization depends, not only on the AlN buffer, but also on the growth rate and the adequacy of the growth temperature to the stoichiometry condition, as shown in Fig. 8. The dominant feature of the PL spectra is no longer at 3.455 eV but at 3.465 ± 0.003 eV. Assuming that these compact GaN layers are under a biaxial-tensile strain of thermal origin, and taking

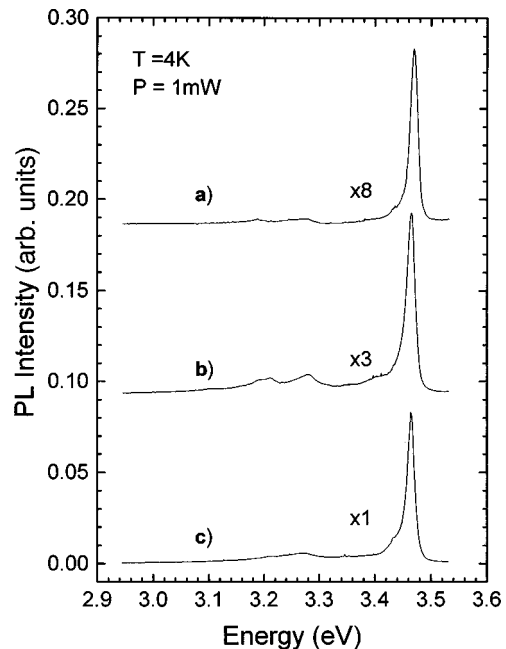


FIG. 8. PL spectra at 4 K from undoped GaN layers grown on optimized AlN buffers: (a) GaN grown at 760 °C at a rate of 0.5 $\mu\text{m}/\text{h}$, (b) GaN grown at 720 °C at a rate of 0.08 $\mu\text{m}/\text{h}$, (c) GaN grown at 740 °C at a rate of 0.08 $\mu\text{m}/\text{h}$.

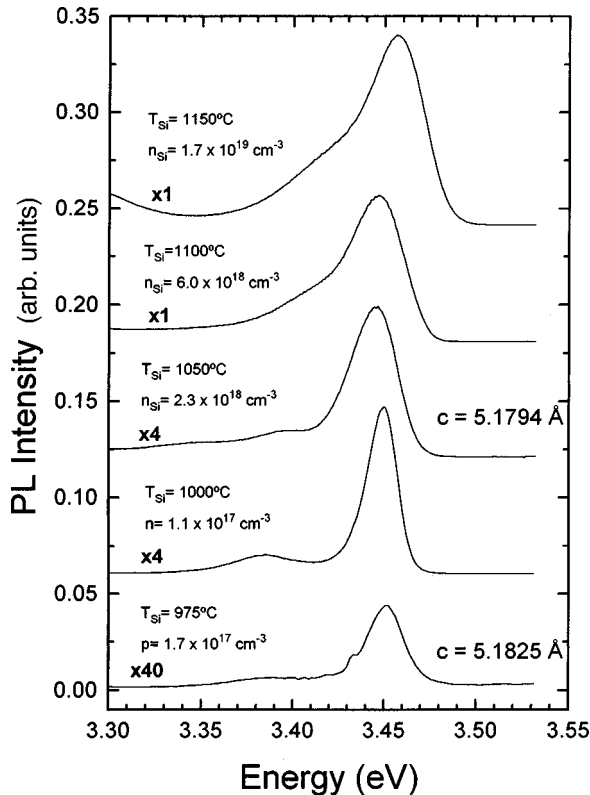


FIG. 9. PL spectra at 4 K of Si-doped GaN layers grown at 760 °C on AlN buffers. Spectra are shifted but they have the same baseline.

into account the improved crystal quality, the emission at 3.465 eV is assigned to the free-exciton A.²³ The peak at 3.455 eV is not much evident in these spectra, perhaps because Si does not diffuse through the AlN buffer, or because it might be masked by the dominant emission. However, if we take the emission at 3.455 eV as a Si-donor-bound exciton, it would give a Si-donor binding energy of 50 meV, following Haynes's rule.²⁶

D. Photoluminescence measurements in Si-doped GaN layers

Photoluminescence spectra were taken in a series of GaN samples doped with Si and grown at 760 °C under stoichiometric conditions on optimized AlN buffers. Figure 9 shows the spectra evolution from low to heavily Si-doped layers, where, within a few millivolts, the energy of the dominant peak is the same and its value coincides with that observed in all undoped layers in Fig. 6. Time-resolved PL measurements in Si-doped samples [Fig. 7(b)] give a similar exponential decay (160 ps) as that of undoped GaN layers where Si diffusion has been observed [Fig. 7(a)]. We conclude that the peak at 3.455 eV is due to donor-bound exciton involving Si donors with an optical binding energy of 50 meV. This value agrees well with previous data reporting a binding energy for the exciton bound to neutral Si donors of 8.6 meV,²⁷ which gives a donor binding energy of 43 meV.²⁶ Emissions at 3.458 eV, reported in Si-doped GaN grown homoepitaxially²⁸ and on sapphire,²⁹ were attributed to donor- or to acceptor-bound excitons, but it seems more probable that these emissions (as well as those in Refs. 24 and 25) be due to an exciton bound to a neutral Si-donor.

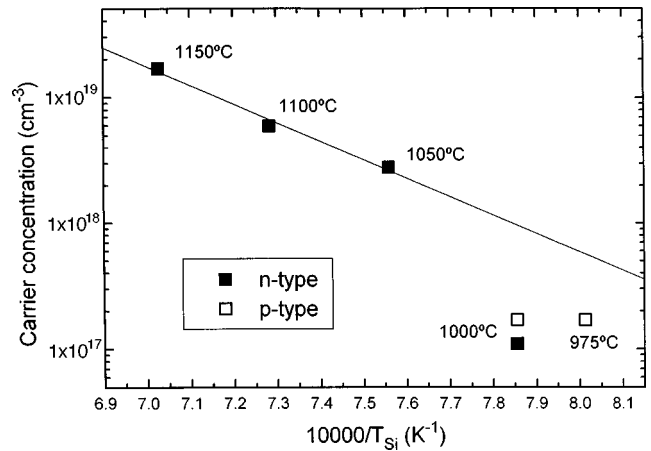


FIG. 10. Hall-carrier concentration in Si-doped GaN layers. For low-doping levels samples show *p*-type conductivity (see text).

The emission at 3.455 eV in Fig. 9 shifts to lower energies with the increasing doping, up to low 10^{18} cm^{-3} , then it blueshifts and broadens markedly for higher doping levels. A similar shift to lower energies, observed in Si-doped GaN/Al₂O₃ for emissions at 3.455 eV (Ref. 30) and at 3.410 eV (at room temperature),³¹ can be due to the relaxation of the residual strain in the layer,^{32,33} or to the presence of a hydrostatic strain due to the incorporation of point defects to the lattice.³⁴ XRD measurements reveal that undoped samples are already under biaxial-tensile strain with $c = 5.1827$ Å, well below the relaxed value of 5.1850 Å, and a progressive reduction of the lattice parameter c , together with a PL peak redshift, take place as the Si-doping increases (Fig. 9), in good agreement with previous data in GaN/AlN/SiC by Perry *et al.*³⁵ The origin of this behavior might be the reduction of the dislocation density, driven by the doping, as pointed out before by Ruvimov *et al.*,³³ that would lead in our case to an increase of the biaxial-tensile strain in the layer. The peak shift to higher energies, for doping levels above 10^{18} cm^{-3} , is a consequence of band filling, whereas the peak broadening is attributed to potential fluctuations due to a random distribution of the Si impurities,³¹ as well as to the band filling.

E. Hall measurements in Si-doped GaN layers

Hall measurements, performed at room temperature in 1- μm -thick Si-doped GaN layers grown at 760 °C on AlN buffers, are shown in Fig. 10. The *n*-type carrier concentration follows a typical exponential dependence with the Si-cell reciprocal temperature for doping levels above 10^{18} cm^{-3} , whereas lower doping levels result in an apparent *p*-type conductivity of the layers due to Al diffusion into the Si substrate, as mentioned earlier. Although 0.5- μm -thick AlN buffer layers were grown at 910 °C, the Hall current is dominated by the *p*-type interface layer for low Si doping levels. Indeed, the layer doped with $T_{\text{Si}} = 1000$ °C shows *p*-type conductivity with annealed In Ohmic contacts, but *n*-type with unannealed Ti/Al (Fig. 10). Electron mobility increases with doping level from very low values (10 $\text{cm}^2/\text{V s}$) to a typical²⁷ value of 100 $\text{cm}^2/\text{V s}$ for 10^{19} cm^{-3} . Low mobilities may arise from *p*-type interface-layer conduction, compensation, or scattering by disloca-

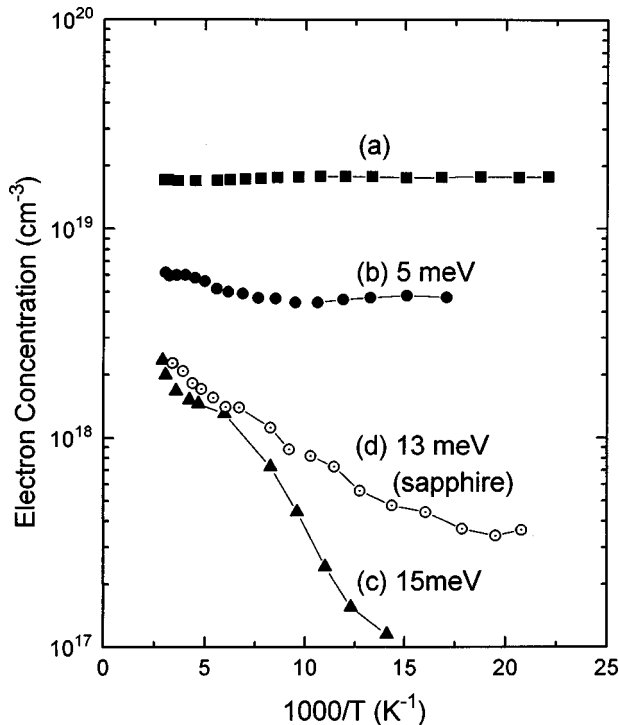


FIG. 11. Temperature-dependent Hall data of Si-doped GaN layers. Curve (d) corresponds to a GaN sample grown by MOVPE on sapphire. Activation energies are derived from the high-temperature region, assuming compensation (E_D/KT).

tions. An increase in Si doping not only overpowers the p -type conduction at the interface, but also enhances the crystal quality. High Si-doping levels have been found to enhance the band-edge luminescence in GaN layers,^{31,36,37} and some authors correlated this improvement to a dislocation-density reduction.³³

Temperature-dependent Hall data in Fig. 11 show a degenerate electron concentration, independent of the temperature, when doping above 10^{19} cm^{-3} (metallic conduction). Decreasing doping densities leads to electron freeze-out and to increasing donor activation energies that follow the equation $E_D = E_{D0} - \alpha N_D^{1/3}$, with α being the screening factor equal to $2.1 \times 10^{-5} \text{ meV cm}$ (Refs. 17 and 20) and N_D the donor concentration. Different values of E_{D0} have been derived from PL data (35 meV) (Ref. 17) in undoped GaN, and from Hall data in Si-doped GaN (29 meV) (Ref. 20) assuming either low or no compensation, and taking N_D as the Hall electron density. However, in the case of compensated samples, the electron density equals $N_D - N_A$ instead of N_D , and the E_{D0} value derived from the above equation might be significantly different. Since the compensation ratio in our samples is unknown, taking N_D as the Hall electron concentration in Fig. 11 gives an E_{D0} value about 45 meV, higher than the above-mentioned values, but very close to the Si-donor optical-binding energy measured from PL experiments (see Sec. III D and Ref. 27).

Different binding energies might be derived depending on the doping level, compensation ratio, measurement technique (PL, Hall, IR absorption) and fitting procedure, so that care must be taken when comparing different data. This fact might well explain the large spread of energies published for Si donors in GaN layers. However, if we consider a donor

concentration in the mid 10^{17} cm^{-3} range and compensated samples (E_D/KT), most authors coincide to assign an E_D value between 13 and 17 meV to Si donors,^{16,20,29,37} and small deviations might arise just from different compensation ratios. Results from undoped samples¹⁷ also give 16 meV. A Si-donor energy of 29 meV, derived from infrared-absorption measurements³⁸ in samples doped to $1.6 \times 10^{17} \text{ cm}^{-3}$, agrees with the Hall data if no compensation is assumed,^{16,17} but most undoped and n -type doped GaN layers are compensated.^{14–16,39} Higher binding energies (62 meV) have been reported in cubic GaN (Ref. 40) and hexagonal GaN (Ref. 41) from Hall measurements. Our results from Hall measurements agree better with smaller Si-donor binding energies, but PL data lead to a higher value (50 meV). An unambiguous determination of this energy is still needed.

Since impurity-band formation starts in GaN for doping levels above 10^{17} cm^{-3} , a reliable donor-activation energy calculation from Hall data should be done for doping levels up to, or below 10^{17} cm^{-3} . However, Hall data from our GaN samples doped in this range are unreliable due to the mentioned effect of the Ga diffusion. Below 130 K, curves (b)–(d) in Fig. 11 tend to flatten as a result of impurity-band conduction that dominates at low temperatures for doping levels above 10^{17} cm^{-3} . Curve (d) shows data from a Si-doped GaN sample grown by MOVPE on sapphire, where no interface problems are expected. This sample has a normal behavior with temperature, in contrast to that found in curve (c). A similar abnormal thermal dependence was previously reported by Kim *et al.* in GaN grown by MBE on β -SiC coated Si(100).⁴⁰ Whether this behavior is related to an interfacial p -type layer conduction or to different conduction mechanisms, more work is needed to ascertain and quantify this point.

F. Positron annihilation spectroscopy in undoped GaN layers

The Doppler broadening of the 511-keV annihilation radiation was recorded as a function of the positron-beam energy in nominally $0.78\text{-}\mu\text{m}$ -thick undoped GaN layers grown at 660, 720, 760, and 780 °C directly on the Si(111) substrates without buffer layers. The shape of the 511-keV line is the momentum distribution of the annihilated electrons. It was described using the conventional low and high electron-momentum parameters S and W .⁴² When positrons annihilate at vacancies, the S parameter increases due to the lower kinetic energies of valence electrons and the W parameter decreases due to missing core electrons.

The S parameter vs the positron-beam energy E is shown in Fig. 12 for all measured samples. The $S(E)$ curve is a superposition of the specific parameter values for different positrons states. The fraction of positrons in each state varies with the beam energy, i.e., the positron stopping depth. At $E = 0 \text{ keV}$ positrons annihilate at the GaN surface. Between 2 and 8 keV positrons stop and annihilate in the GaN overlayer. Above 10 keV an increasing fraction of positrons penetrate to the Si substrate and the S parameter shoots up towards the Si-specific value $S_{\text{Si}} = 0.520 \pm 0.001$.

The level of the plateau from 2 to 8 keV characterizes the corresponding GaN layer. In the layer grown at 660 °C, the level is very close to that found for free positrons in the GaN

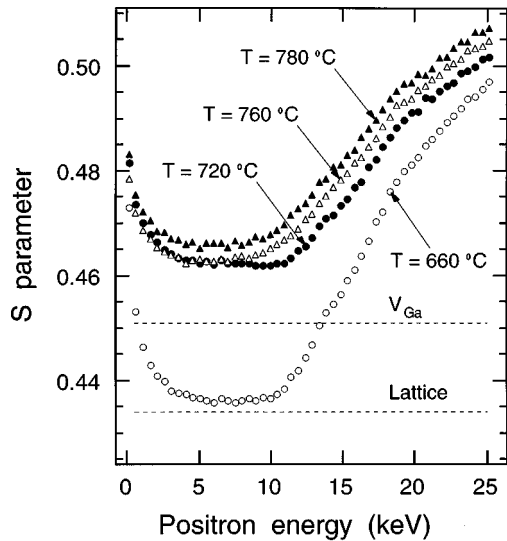


FIG. 12. The low electron-momentum parameter S vs positron-beam energy in undoped GaN/Si(111) grown at various temperatures. The specific S values for free positrons in the GaN lattice and trapped positrons in Ga vacancies are also marked.

lattice,⁴³ $S_B = 0.434 \pm 0.001$. In the other three layers the plateau levels are much higher, even above the specific values of the Ga vacancy determined earlier.⁴³ This is a clear indication of vacancy-type defects in the layers.

The $W(E)$ curves (not shown) are nearly the mirror images for the $S(E)$ curves. The specific value for the GaN lattice is $W_B = 0.0690 \pm 0.002$, and the plateau values are 0.0681, 0.0577, 0.0576, and 0.0565 for the growth temperatures 660, 720, 760, and 780 °C, respectively. In the Si substrate the W value is very low, $W_{Si} = 0.0263 \pm 0.002$ due to the absence of the Ga 3d electrons.

We use the S - W plot^{42,43} to illustrate the positron states and to estimate the specific (S_D, W_D) values for the defect that traps positrons in the layers. The ($S(E), W(E)$) points have been marked on the plot in Fig. 13. The surface effects have been dropped out by skipping the points with $E < 5$ keV. The positions of the positron states in the defect-free GaN lattice and in the Si substrate have been indicated, too. For the sake of clarity, the plateau values averaged from 5 to 8 keV have been marked by bigger symbols. One can see that all the plateau points fall on one line that goes through the “GaN Lattice” point. This means that the annihilations in the plateau regions arise from superpositions of two states: the free positrons in the lattice and the trapped positrons in the defects. The defect is the same in all layers and the specific defect state (S_D, W_D) must lie on this line, too. If we extrapolate the (S, W) points of high E through the Si-substrate state, we get a second line. The crossing point (“Vacancy cluster”) is the positron state in the common defect present in all layers. Now all the experimental points fall inside the triangle “GaN Lattice–Vacancy cluster–Si” meaning that the experimental data in Fig. 13 can be explained as superpositions of annihilations in these three positron states.

The defect that traps positrons in the GaN layers has the normalized specific values $S_D/S_B = 1.10 \pm 0.002$ and $W_D/W_B = 0.75 \pm 0.003$. Compared with the Ga vacancy

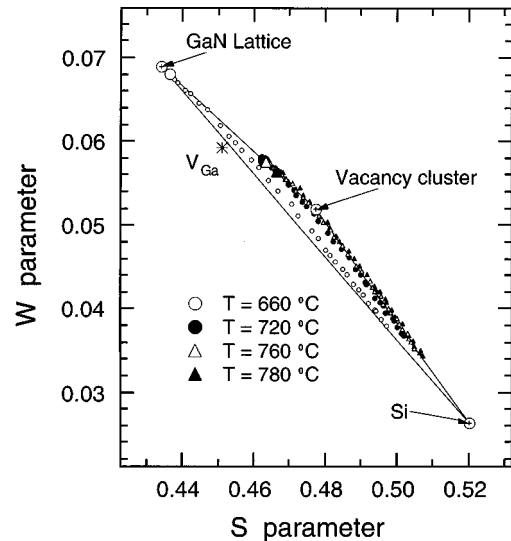


FIG. 13. The S - W plot for the GaN/Si(111) layers after dropping out the surface effects. For the sake of clarity, the layer characteristic plateau values have been marked by bigger symbols. The open circles with a central cross denote the positron-annihilation states.

($S_{V_{Ga}}/S_B = 1.038$, $W_{V_{Ga}}/W_B = 0.86$) also marked in Fig. 13, we conclude that the defect is far from being a monovacancy. The decoration of a Ga vacancy by a Si impurity cannot change much the specific (S, W) values, as the Si atom occupies a substitutional site in the second nearest shell. Therefore, the defect cannot be a V_{Ga} -Si pair. The high S_D and low W_D values of the defect suggest an open volume at least twice that of a monovacancy, i.e., the defect is a vacancy cluster. Using a trapping coefficient of 10^{15} s^{-1} we estimate the vacancy-cluster concentration to be $< 10^{17}$, 5×10^{17} , 8×10^{17} , and $1 \times 10^{18} \text{ cm}^{-3}$ in the layers grown at 660, 720, 760, and 780 °C, respectively.

The SIMS results in Figs. 4 and 5 clearly demonstrate the strong Si diffusion across the GaN/Si interface when no buffer layer exists. The Si profile penetrates 100–300 nm to the GaN side. Looking carefully at the PAS results, we see that the $S(E)$ values at the interface regions ($E = 10$ –14 keV) increase rapidly above the plateau levels in Fig. 12, but the corresponding points in the S - W plot of Fig. 13 still continue to follow the “GaN Lattice–Vacancy cluster” line. This means that at the interface regions the positrons encounter vacancy-cluster concentrations that are 5–10 times higher than in the plateau regions.

Vacancies are known to be vehicles for substitutional atoms. Here PAS does not detect Ga vacancies nor V_{Ga} -Si pairs. Instead, vacancy clusters are observed that are evidently stable traces left by diffusion processes during the layer growth. The Ga vacancy has been identified in metal-organic chemical-vapor deposition layers grown on sapphire and their concentration has been seen to correlate with the yellow luminescence intensity.⁴³ The PL results from the present layers, with or without AlN buffers, show no traces of the yellow band, either at low temperatures or at room temperature, whether they are undoped or Si-doped, and thus, these results are parallel with the absence of the Ga vacancy signal in PAS measurements.

IV. SUMMARY

In summary, we have studied the optical and transport properties of undoped and Si-doped GaN grown on Si(111) by plasma-assisted MBE. When GaN layers are compact (grown near stoichiometry) there is a significant residual strain (biaxial tensile) of thermal origin. We identify the excitonic emission bound to neutral Si donors having a binding energy of some 50 meV. Undoped GaN layers grown below 660 °C are always *n* type, being the donor species most likely V_N or complexes involving these vacancies. However, growth temperatures above 660 °C promote the diffusion of Ga into the Si substrate and of Si into the GaN layer, making

Hall measurements unreliable for undoped and lightly doped samples. PAS detects vacancy clusters as a result of the strong interdiffusion across the GaN/Si interface without a buffer layer. Ga vacancies are not observed in these layers and they do not show any trace of yellow emission.

ACKNOWLEDGMENTS

E.C., M.A.S.-G., D.B., F.J.S., F.C., P.Y., and E.M. wish to acknowledge the financial support provided by CICYT Project No. TIC95-0770 and by the EU ESPRIT LTR 20968 (Laquani). We also acknowledge fruitful discussions with C. T. Foxon and J. W. Orton.

*Permanent address: Dpt. TSC Ing. Telemática, ETSIT, Univ. Valladolid, Spain.

- ¹B.-C. Chung and M. Gershenson, *J. Appl. Phys.* **72**, 651 (1992).
- ²J. Neugebauer and C. G. Van de Walle, *Phys. Rev. B* **50**, 8067 (1994).
- ³P. Boguslawski, E. L. Briggs, and J. Bernholc, *Phys. Rev. B* **51**, 17 255 (1995).
- ⁴S. Nakamura, M. Senoh, S. Nagahama, N. Iwasa, T. Yamada, T. Matsushita, Y. Sugimoto, and H. Kiyoku, *Appl. Phys. Lett.* **69**, 4056 (1996).
- ⁵X. Zhang, D. Walker, A. Saxler, P. Kung, J. Xu, and M. Razeghi, *Electron. Lett.* **32**, 1622 (1996).
- ⁶J. P. Bergman, T. Lundström, B. Monemar, H. Amano, and I. Akasaki, *Appl. Phys. Lett.* **69**, 3456 (1996).
- ⁷T. Kimoto, A. Yamashita, A. Ito, and H. Matsunami, *Jpn. J. Appl. Phys. Part 1* **32**, 1045 (1993).
- ⁸Y. C. Wang, R. F. Davis, and J. A. Edmond, *J. Electron. Mater.* **20**, 289 (1991). See also C. F. Young, K. Xie, E. H. Poindexter, G. J. Gerardi, and D. J. Keeble, *Appl. Phys. Lett.* **70**, 1868 (1997).
- ⁹M. A. Sánchez-García, E. Calleja, E. Monroy, F. J. Sánchez, F. Calle, E. Muñoz, and R. Beresford, *J. Cryst. Growth* **183**, 23 (1998).
- ¹⁰M. A. Sánchez-García, E. Calleja, F. J. Sánchez, F. Calle, E. Monroy, D. Basak, E. Muñoz, C. Villar, A. Sanz-Hervás, M. Aguilar, J. J. Serrano, and J. M. Blanco, *J. Electron. Mater.* **27**, 276 (1998), special issue on III-Nitrides and SiC.
- ¹¹E. Calleja, M. A. Sánchez-García, E. Monroy, F. J. Sánchez, E. Muñoz, A. Sanz-Hervás, C. Villar, and M. Aguilar, *J. Appl. Phys.* **82**, 4681 (1997).
- ¹²D. C. Look, D. C. Reynolds, W. Kim, O. Aktas, A. Botchkarev, A. Salvador, and H. Morkoç, *J. Appl. Phys.* **80**, 2960 (1996).
- ¹³R. J. Molnar, T. Lei, and T. D. Moustakas, *Appl. Phys. Lett.* **62**, 72 (1993).
- ¹⁴D. L. Rode and D. K. Gaskill, *Appl. Phys. Lett.* **66**, 1972 (1995).
- ¹⁵L. B. Rowland, K. Doverspike, and D. K. Gaskill, *Appl. Phys. Lett.* **66**, 1495 (1995).
- ¹⁶D. K. Gaskill, A. E. Wickenden, K. Doverspike, B. Tadayon, and L. B. Rowland, *J. Electron. Mater.* **24**, 1525 (1995).
- ¹⁷B. K. Meyer, D. Volm, A. Graber, H. C. Alt, T. Detchprohm, A. Amano, and I. Akasaki, *Solid State Commun.* **95**, 597 (1995). See also S. Fisher, C. Wenzel, E. E. Haller, and B. K. Meyer, *Appl. Phys. Lett.* **67**, 1298 (1995).
- ¹⁸D. Basak, M. Verdú, M. T. Montojo, M. A. Sánchez-García, F. J. Sánchez, E. Muñoz, and E. Calleja, *Semicond. Sci. Technol.* **12**, 1654 (1997).

- ¹⁹Activation energies, diffusion coefficients and solubilities for Ga and Al in silicon are taken from A. G. Milnes, *Deep Impurities in Semiconductors* (Wiley, New York, 1973), and references therein.
- ²⁰D. C. Look and R. J. Molnar, *Appl. Phys. Lett.* **70**, 3377 (1997).
- ²¹F. Calle, F. J. Sánchez, J. M. G. Tijero, M. A. Sánchez-García, E. Calleja, and R. Beresford, *Semicond. Sci. Technol.* **12**, 1396 (1997).
- ²²M. A. Sánchez-García, E. Calleja, F. Calle, F. J. Sánchez, E. Monroy, J. M. G. Tijero, R. Beresford, A. Sanz-Hervás, C. Villar, J. J. Serrano, and J. M. Blanco (unpublished).
- ²³D. Volm, K. Oettinger, T. Streibl, D. Kovalev, M. Ben-Chorin, J. Diener, B. K. Meyer, J. Majewski, L. Eckey, A. Hoffmann, H. Amano, Y. Akasaki, K. Hiramatsu, and T. Detchprohm, *Phys. Rev. B* **53**, 16 543 (1996).
- ²⁴M. Godlewski, J. P. Bergman, B. Monemar, U. Rossner, and A. Barski, *Appl. Phys. Lett.* **69**, 2089 (1996).
- ²⁵A. Otani, K. S. Stevens, and R. Beresford, *Appl. Phys. Lett.* **65**, 61 (1995).
- ²⁶J. R. Haynes, *Phys. Rev. Lett.* **4**, 361 (1960).
- ²⁷A. E. Wickenden, L. B. Rowland, K. Doverspike, D. K. Gaskill, J. A. Freitas, D. S. Simons, and P. H. Chi, *J. Electron. Mater.* **24**, 1547 (1995).
- ²⁸F. A. Ponce, D. P. Bour, W. Götz, N. M. Johnson, H. I. Helava, I. Grzegory, J. Jun, and S. Porowski, *Appl. Phys. Lett.* **68**, 917 (1996).
- ²⁹W. Götz, N. M. Johnson, C. Chen, H. Liu, C. Kuo, and W. Imler, *Appl. Phys. Lett.* **68**, 3144 (1996).
- ³⁰M. Leroux, B. Beaumont, N. Grandjean, P. Lorenzini, S. Haffouz, P. Vennéguès, J. Massies, and P. Gibart, *Mat. Ser. Ing. B* (to be published).
- ³¹E. F. Schubert, I. D. Goepfert, W. Grieshaber, and J. M. Redwing, *Appl. Phys. Lett.* **71**, 921 (1997).
- ³²In-Hwan Lee, In-Hoon Choi, C. R. Lee, and S. K. Noh, *Appl. Phys. Lett.* **71**, 1359 (1997).
- ³³S. Ruvimov, Z. Liliental-Weber, T. Suski, J. W. Ager, J. Washburn, J. Krüger, C. Kisielowski, E. R. Weber, H. Amano, and I. Akasaki, *Appl. Phys. Lett.* **69**, 990 (1996).
- ³⁴C. Kisielowski, J. Krüger, S. Ruvimov, T. Suski, J. W. Ager, E. Jones, Z. Liliental-Weber, M. Rubin, E. Weber, M. D. Bremser, and R. F. Davis, *Phys. Rev. B* **54**, 17 745 (1996).
- ³⁵W. G. Perry, T. Zheleva, M. D. Bremser, R. F. Davis, W. Shan, and J. J. Song, *J. Electron. Mater.* **26**, 224 (1997).
- ³⁶S. Nakamura, T. Mukai, and S. Senoh, *Jpn. J. Appl. Phys., Part 1* **31**, 2883 (1992).
- ³⁷P. Hacke, A. Maekawa, N. Koide, K. Hiramatsu, and N. Sawaki,

- Jpn. J. Appl. Phys., Part 1 **33**, 6443 (1994).
- ³⁸Y. J. Wang, R. Kaplan, H. K. Ng, K. Doverspike, D. K. Gaskill, T. Ikedo, I. Akasaki, and H. Amano, J. Appl. Phys. **79**, 8007 (1996).
- ³⁹Gyu. Chul Yi and B. W. Wessels, Appl. Phys. Lett. **69**, 3028 (1996).
- ⁴⁰J. G. Kim, A. C. Frenkel, H. Liu, and R. M. Park, Appl. Phys. Lett. **65**, 91 (1994).
- ⁴¹J. C. Zolper, M. H. Crawford, S. J. Pearton, C. R. Abernathy, C. B. Vartuli, C. Yuan, and R. A. Stall, J. Electron. Mater. **25**, 839 (1996). See also Appl. Phys. Lett. **70**, 2729 (1997).
- ⁴²P. Hautojärvi and C. Corbel, in *Positron Spectroscopy of Solids*, edited by A. Dupasquier and A. P. Mills, Jr. (IOS, Amsterdam, 1995).
- ⁴³K. Saarinen, T. Laine, S. Kuisma, J. Nissilä, L. Dobrzynski, J. M. Baranowski, K. Pakula, R. Stepniewski, M. Wojdak, A. Wyszomolek, T. Suski, M. Leszczynski, I. Grzegory, and S. Porowski, Phys. Rev. Lett. **79**, 3033 (1997).